

Supporting information

Control of interpenetration in S-containing metal-organic frameworks for selective separation of transition metal ions

Guang-Sheng Yang, Zhong-Ling Lang, Hong-Ying Zang, Ya-Qian Lan,* Wen-Wen He,
Xiao-Liang Zhao, Li-Kai Yan, Xin-Long Wang and Zhong-Min Su*

Institute of Functional Material Chemistry; Faculty of Chemistry, Northeast Normal University, Changchun, 130024, People's Republic of China; E-mail:
lanyq176@nenu.edu.cn; zmsu@nenu.edu.cn

S1. Materials and instrumentation

All chemical materials were purchased from commercial sources and used without further purification. 3,4-Dimethylthieno[2,3-b]thiophene-2,5-dicarboxylic acid (H_2DMTDC),¹ **MOF-5**² and **IRMOF-3**³ were synthesized according to the previous references. The FT-IR spectra were recorded from KBr pellets in the range of 4000–400 cm^{-1} on a Mattson Alpha-Centauri spectrometer. The phase purities of the bulk samples were identified by X-ray powder diffraction on a Rigaku, Rint 2000 diffractometer. The C, H, and N elemental analyses were conducted on a Perkin-Elmer 240C elemental analyzer. TGA was performed on a Perkin–Elmer TG-7 analyzer heated from room temperature to 800 °C at a ramp rate of 5 °C/min under nitrogen. ICP was measured by ICP-9000(N+M) (USA Thermo Jarrell-Ash Corp).

S2. Synthesis of Compounds

Synthesis of IFMC-27

3,4-Dimethylthieno[2,3-b]thiophene-2,5-dicarboxylic acid (H_2DMTDC) (0.0256 g, 0.10 mmol) and zinc nitrate hexahydrate (0.178 g, 0.60 mmol) were dissolved in 10 mL of *N,N'*-dimethylformamide (DMF) in a 20 mL a Teflon reactor. The reaction mixture was heated in an oven at 100 °C for 12 h. The cubic crystals were isolated and washed by anhydrous DMF. Anal. Calcd. For $\text{C}_{48}\text{H}_{60}\text{N}_6\text{O}_{19}\text{S}_6\text{Zn}_4$: C, 38.98; H, 4.09; N, 5.68. Found: C, 38.52; H, 4.23; N, 5.35. The powder X-ray diffraction pattern of the bulk sample matched that of the pattern simulated from the single crystal structure of **IFMC-27**. Chemical formula of **IFMC-27** was determined by elemental analysis and thermogravimetric analysis combining with the X-ray single-crystal diffraction analysis.

Synthesis of IFMC-28

H_2DMTDC (0.0128 g, 0.05 mmol) and zinc nitrate hexahydrate (0.089 g, 0.30 mmol) were dissolved in 10 mL of *N,N'*-diethylformamide (DEF) in a 20 mL a Teflon reactor. The reaction mixture was heated in an oven at 100 °C for 48 h to yield large, cube-shaped crystals. The cubic crystals were isolated and washed by anhydrous DEF. Anal. Calcd. For $\text{C}_{65}\text{H}_{95}\text{N}_7\text{O}_{20}\text{S}_6\text{Zn}_4$: C, 44.65; H, 5.48; N, 5.61. Found: C, 44.90; H, 5.88; N, 5.38. The powder X-ray diffraction pattern of the bulk sample matched that of the pattern simulated from the single crystal structure of **IFMC-28**. Chemical formula of **IFMC-28** was determined by elemental analysis and thermogravimetric analysis combining with the X-ray single-crystal diffraction analysis.

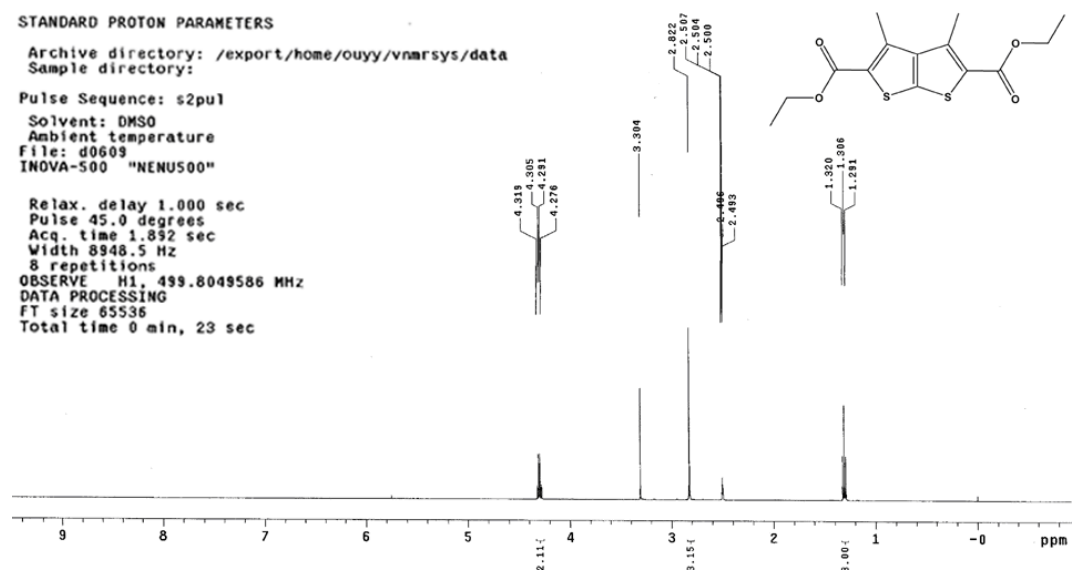


Fig. S1 The ^1H NMR signal of diethyl 3,4-dimethylthieno[2,3-b]thiophene-2,5-dicarboxylate, DMTDC-(C₂H₅)₂.

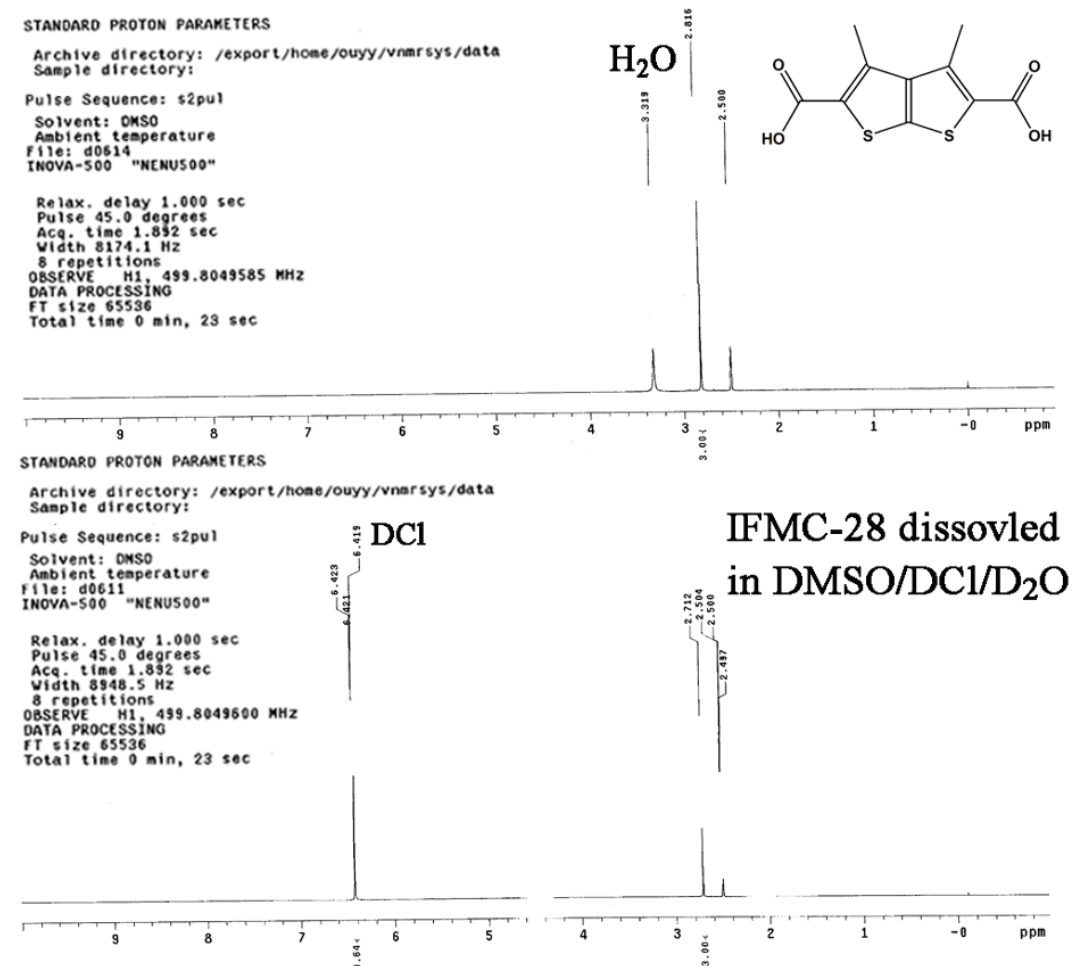


Fig. S2 The ^1H NMR signals of 3,4-dimethylthieno[2,3-b]thiophene-2,5-dicarboxylic acid (H₂DMTDC) in d_6 -DMSO and **IFMC-28** dissolving in d_6 -DMSO/DCl/D₂O.

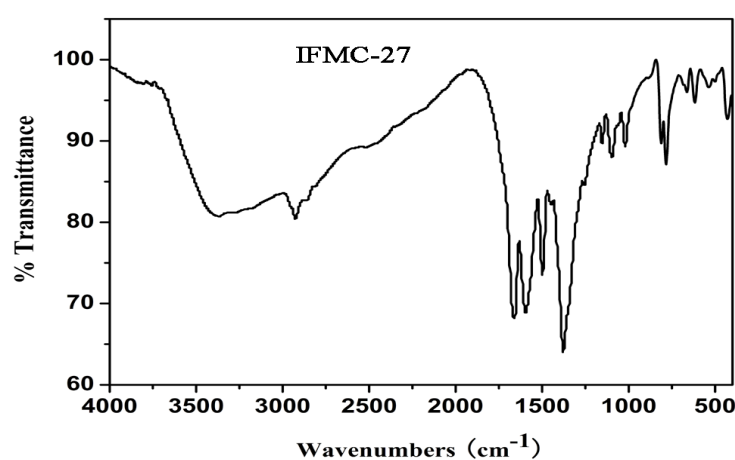


Fig. S3 IR spectrum of IFMC-27.

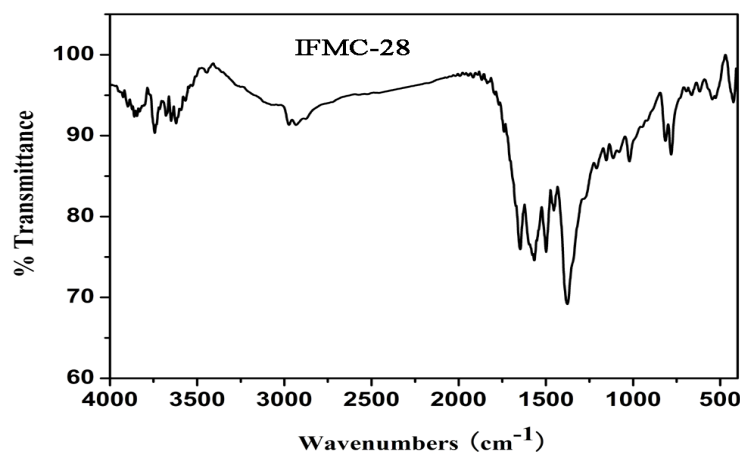


Fig. S4 IR spectrum of IFMC-28.

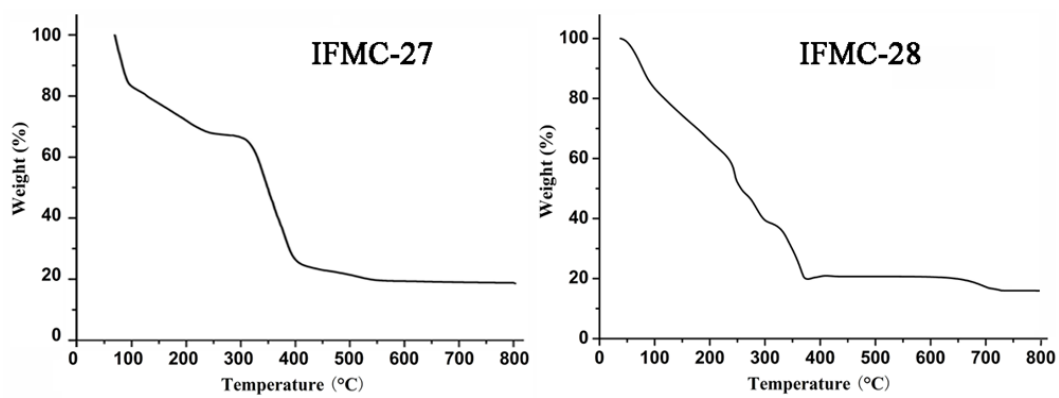


Fig. S5 TGA curves of IFMC-27 and IFMC-28.

S3. Single-crystal X-ray structure determination and refinement details

Single-crystal X-ray structure determination: Crystal data for **DMTDC-C₂H₅**, **IFMC-27** and **IFMC-28** were recorded on a Bruker Apex CCD II area-detector diffractometer with graphite-monochromated Mo K α radiation ($\lambda = 0.71069 \text{ \AA}$) at 293 K. Absorption corrections were applied using multi-scan technique. Their structures were solved by direct method of SHELXS-97 and refined by full-matrix least-square techniques using the SHELXL-97 program.⁴ Because guest solvent molecules (DMF or DEF) in the frameworks of **IFMC-27** and **IFMC-28** were highly disordered, the diffused electron densities resulting from them were removed by the SQUEEZE routine in PLATON⁵ and the platon.sqf files were attached to the CIF files. Due to the weak quality of crystal data, the electron number in the void obtained from the platon.sqf files have not been used to calculate the guest solvent molecules crystallizing in the pore of **IFMC-27** and **IFMC-28**. These molecules are estimated by TGA analysis combining with element analysis, and the results were introduced to the CIF files. Details for structural analysis were summarized in Table S1. CCDC 902283–902285 contains the supplementary crystallographic data for this paper. This data can be obtained free of charge from the Cambridge Crystallographic Data Centre via www.ccdc.cam.ac.uk/data_request/cif.

Table S1 Details for structural analysis of DMTDC-C₂H₅, IFMC-27 and IFMC-8.

Compound	DMTDC-C ₂ H ₅	IFMC-27	IFMC-28
Formula	C ₁₄ H ₁₆ O ₄ S ₂	C ₄₈ H ₆₀ O ₁₉ N ₆ S ₆ Z	C ₆₅ H ₉₅ O ₂₀ N ₇ S ₆ Z
Formula weight	312.39	1478.86	1748.32
Crystal system	Triclinic	Orthorhombic	Cubic
Space group	<i>P</i> -1	<i>Pna</i> 2 ₁	<i>Fm</i> -3 <i>m</i>
<i>a</i> /Å	7.542(3)	18.095(4)	29.171(7)
<i>b</i> /Å	8.464(5)	14.470(5)	29.171(7)
<i>c</i> /Å	13.006(6)	22.069(7)	29.171(7)
α /°	102.844(3)	90.00	90.00
β /°	100.097(3)	90.00	90.00
γ /°	107.616(4)	90.00	90.00
<i>V</i> /Å ³	744.8(7)	5778(3)	24823(7)
<i>Z</i>	2	4	8
D _{calcd.} [g cm ⁻³]	1.393	1.70	0.936
μ /mm ⁻¹	0.367	1.935	0.910
F(000)	328	3032	7280
Observed reflection /unique	4022/2696	28873/8931	21877/710
Flack parameter	none	0.52(2)	none
<i>R</i> _{int}	0.0839	0.1403	0.2492
Goodness-of-fit on F ²	1.042	0.898	1.117
<i>R</i> ₁ , <i>wR</i> ₂ [I > 2σ(I)]	0.0493, 0.1249	0.0652, 0.1113	0.0821, 0.2098
<i>R</i> ₁ , <i>wR</i> ₂ (all data)	0.0706, 0.1366	0.1277, 0.1286	0.1228, 0.2369

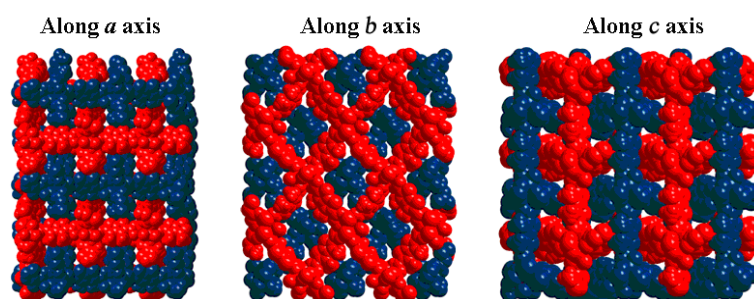


Fig. S6 The space-filling diagrams of IFMC-27 along different directions.

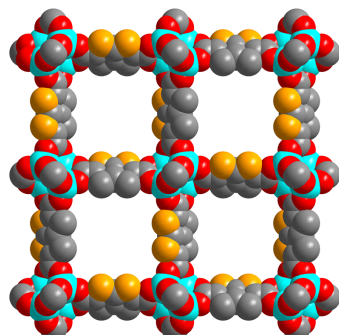


Fig. S7 The space-filling diagram of IFMC-28 along *a*, *b* and *c* axes.

S4. Gas sorption experiments

The N₂ sorption measurements were performed on an automatic volumetric adsorption equipment (Belsorp mini II). Before gas adsorption measurements, the sample was immersed in CH₂Cl₂ for 3 days to remove the nonvolatile solvates (DMF or DEF). The sample was collected by decanting and activated by drying under a dynamic vacuum at 80 °C overnight. Before the measurement, the sample was dried again by using the ‘outgas’ function of the surface area analyzer for 12 h at 150 °C.

Table S2 Gas sorption details of IFMC-27, IFMC-28 and Cu²⁺@IFMC-28.

MOFs	V _m (STP, cm ³ g ⁻¹)	S _{BET} (m ² /g)	S Langmuir (m ² /g)	V _t (cm ³ /g)
IFMC-27	99	430	500	0.1934
IFMC-28	353	1540	1843	0.6583
Cu²⁺@IFMC-28	195	849	1035	0.4252

S5. PXRD patterns related to this work.

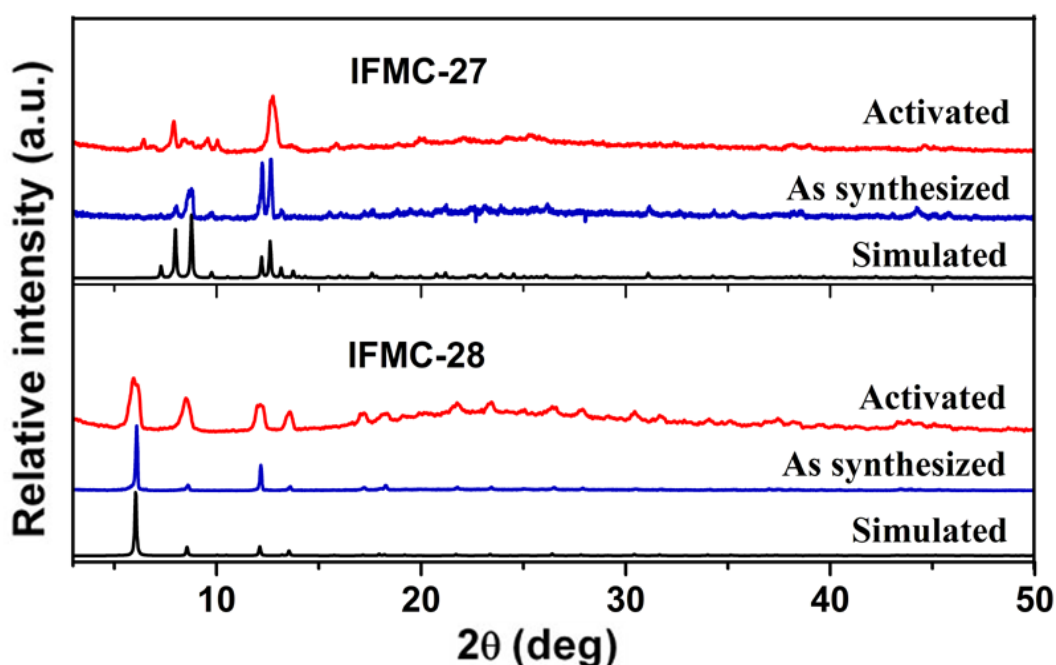


Fig. S8 Powder XRD patterns of IFMC-27 and IFMC-28.

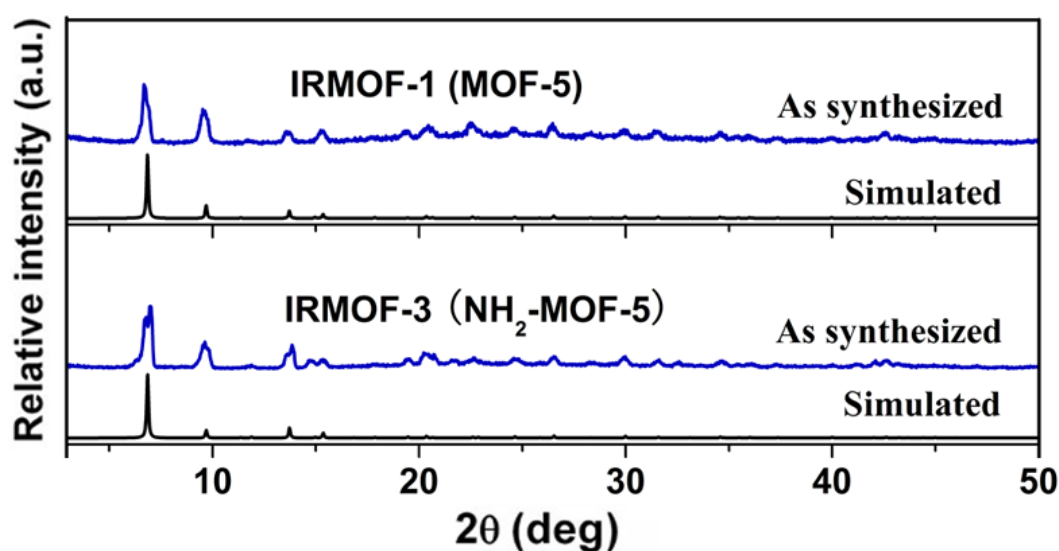


Fig. S9 Powder XRD patterns of MOF-5 and IRMOF-3.

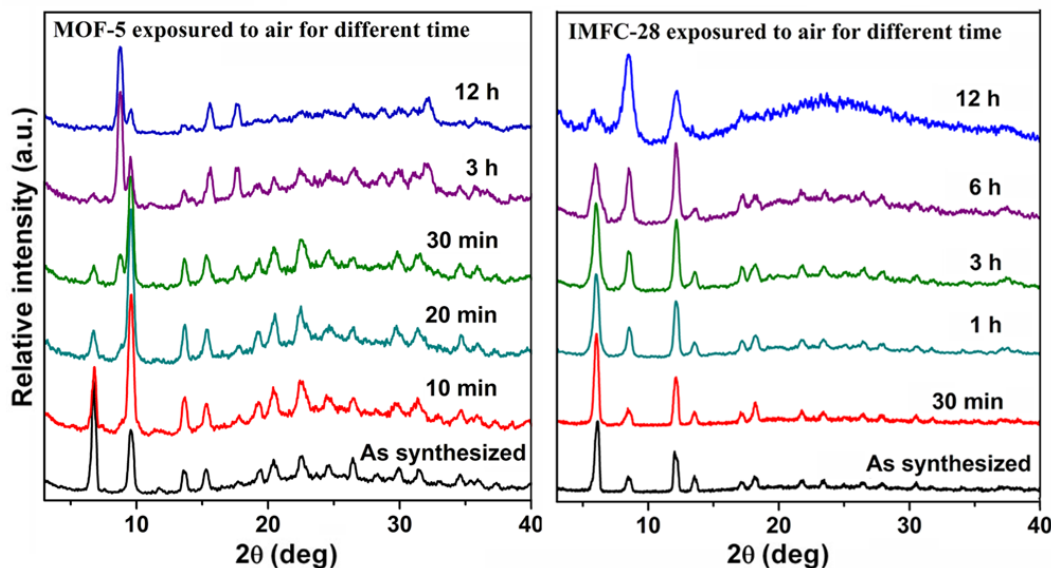


Fig. S10 Powder XRD patterns of stability comparison between **IFMC-28** and **MOF-5** exposed to air.

Air stability comparison of **IFMC-28** and **MOF-5** was studied by PXRD experiments. Exposure of fresh prepared **IFMC-28** to air for 6 h did not result in appearance of new peaks in the powder X-ray diffraction pattern and the relative intensity have no large change. Under the same condition, exposing the fresh prepared **MOF-5** to air for 30 min, a new peak at $2\theta = 8.9^\circ$ appears and the relative intensity of it gradually increases after further exposure, suggesting formation of **MOF-69C**.⁶ These results indicate that hydrophobic CH_3 - groups might effectively improve the moisture resistance of Zn_4O SBUs in MOF.⁷

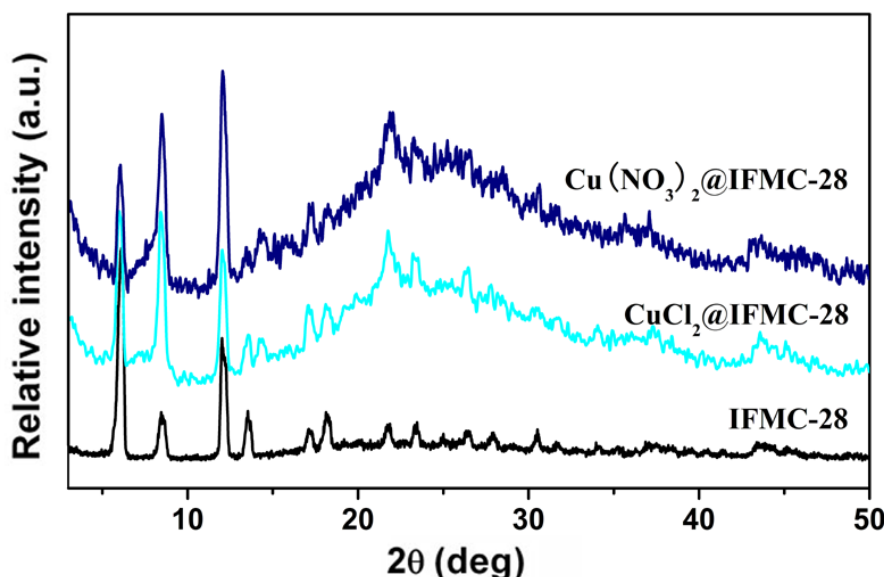


Fig. S11 Powder XRD patterns of **IFMC-28** immersed in DMF solution of CuCl_2 and $\text{Cu}(\text{NO}_3)_2$.

S6. Metal ion adsorption and separation

Single metal ion adsorption in **IFMC-28**

The activated **IFMC-28** (0.03 g) was immersed in 10 mL, 0.1 mmol/L $M(NO_3)_2 \cdot nH_2O$ ($M = Cu^{2+}, Co^{2+}, Ni^{2+}, Mg^{2+}, Cd^{2+}, Pb^{2+}$ or Mn^{2+}) DMF solution for 4 hours. The crystals were filtrated and dissolved in concentrated HNO_3 at 180 °C for 1 day. Then the solution was clarified by filtration and analysed by ICP-9000(N+M) to determinate the ratio of metal ions.

Selective metal ion adsorption in **IFMC-28**, **IRMOF-1** and **IRMOF-3**

Every activated MOF (0.03 g) was immersed in 10 mL metal ion DMF solvent with the same concentration (0.1 mmol/L) of $Cu(NO_3)_2 \cdot 6H_2O$, $Co(NO_3)_2 \cdot 6H_2O$ and $Ni(NO_3)_2 \cdot 6H_2O$ for 4 hours. The crystals were filtrated and dissolved in concentrated HNO_3 at 180 °C for 1 day. Then the solution was filtrated and analysed by ICP-9000(N+M) to determine the metal ion concentration.

MOF-based separation column

This separation column (80 mm × 5 mm) was obtained by filling the pulverized crystals (particle size 2~20 µm) of **IFMC-28** into a glass dropper, and a little of asbestos was placed at the bottom of this glass dropper to prevent the crystals flowing out.

Table S3 ICP results for single metal ion adsorption in **IFMC-28**

Metal ions (M)	M/Zn Mass ratio (experimental)	M/Zn Mol ratio (calculation)
Cu	59.8/70.8	0.87
Pb	16.3/73.5	0.07
Co	1.26/70.4	0.02
Ni	0.70/73.8	0.01
Mn	0.42/69.2	0.0072
Cd	0.81/71.4	0.0066
Mg	0.15/74.9	0.0054

Table S4 ICP results for selective metal ion adsorption in **IFMC-28**, **IRMOF-1** and **IRMOF-3**

	IFMC-28	MOF-5	IRMOF-3
Cu/Zn Mass ratio	60.1/72.8	6.40/91.5	1.48/93.2
Cu/Zn Mol ratio	0.85/1	0.072/1	0.016
Co/Zn Mass ratio	1.66/72.8	2.72/91.5	1.18/93.2
Co/Zn Mol ratio	0.025/1	0.033/1	0.014
Ni/Zn Mass ratio	0.96/72.8	1.56/91.5	0.67/93.2
Ni/Zn Mol ratio	0.015/1	0.020/1	0.008

S7. Computational details

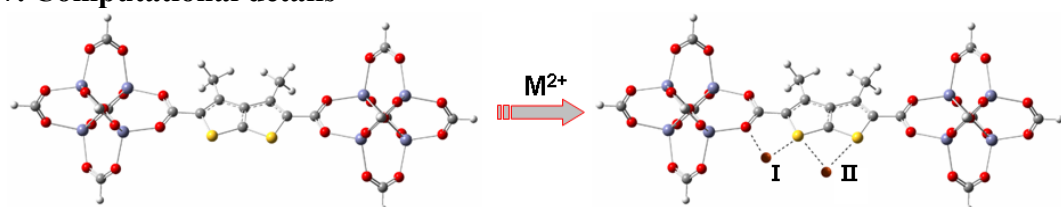


Fig. S12 The optimized model for **IFMC-28** (left) and two possible adsorption sites (right).

An ideal model was truncated for forecasting the stability of the two cases by density functional theory calculations. All species here were calculated with BP86 [8-9] generalized gradient approximations and VWN [10] local density functional, triple- ζ plus polarization (TZP) Slater type orbital basis sets, and the numerical integration parameter 6.0, as implemented in the Amsterdam Density Functional (ADF2010) package [11-13]. The core shells {C, O: (1s)², S: (1s2s2p)¹², Co, Cu, Zn: (1s2s2p3s3p)¹⁹} were kept frozen and were described by means of single Slater functions. Relativistic corrections were included by means of the ZORA formalism.^[14-16] All the structures were optimized in the presence of a continuous model solvent by means of the conductor-like screening model (COSMO).^[17-18] The solute dielectric constant was set to 37 (DMF). The van der Waals radii for the atoms in the framework, which actually define the cavity in the COSMO, are 1.08, 1.49, 1.40, 1.82, 1.92, 1.86 and 2.10 Å for H, C, O, S, Co, Cu, and Zn, respectively.^[19] Our calculation models consist of a truncated MOF framework and a metal ion, the chemical formulas for the models are labeled as **Cu²⁺@IFMC-28** and **Co²⁺@IFMC-28**, respectively. As the experiments have proved that the **IFMC-28** framework is stable and rigid, thus full geometry optimizations (assuming C_{2v} symmetry) were carried out firstly on the **IFMC-28** with BP86 method. Then keeping the equilibrium geometries of **IFMC-28** fixed, two adsorption sites (O···M···S and S···M···S, in Fig. S10) on **IFMC-28** for Cu²⁺ and Co²⁺ were optimized at the same level. In addition, The interaction energy (ΔE) of the metal ion M²⁺ with SMOF is calculated as follows:

$$\Delta E (\text{IFMC-28 : M}^{2+}) = E_{\text{tot(M@IFMC-28)}} - E_{\text{tot(IFMC-28)}} - E_{\text{tot(M}^{2+}\text{)}}$$

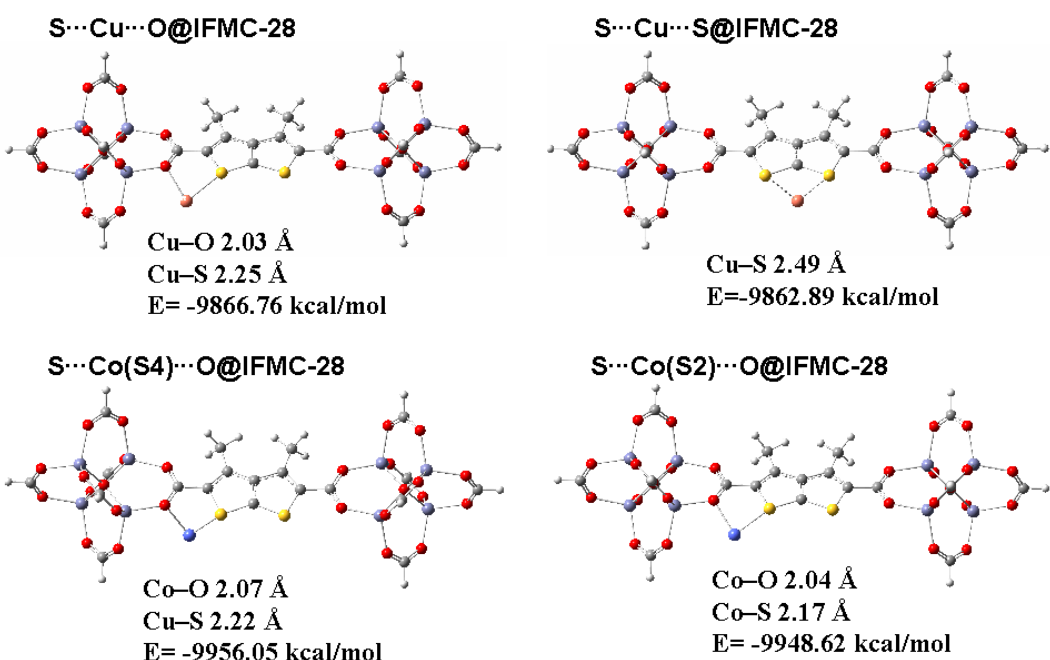


Fig. S13 The calculated results by ADF including bond length and total energy of every optimized model.

The calculated important geometry parameters are labeled at the corresponding position in Fig. S11. DFT calculations predict that Cu^{2+} ions chelated between in $\text{S}\cdots\text{O}$ ($R_{\text{Cu}-\text{O}} = 2.03 \text{ \AA}$, $R_{\text{Cu}-\text{S}} = 2.25 \text{ \AA}$) is slightly more stable than that in $\text{S}\cdots\text{S}$ site ($R_{\text{Cu}-\text{S}} = 2.49 \text{ \AA}$) with 3.87 kcal/mol. In addition, the $\text{S}\cdots\text{Co}\cdots\text{O}$ chelated coordination model also have been optimized at the same level. Two configurations are considered for the Co species, i.e. doublet (S2) and quartet (S4). The calculation results indicate that **Co(S4)-IFMC-28** ($E_{\text{tot}} = -9956.05 \text{ kcal/mol}$) is more stable than **Co(S2)-IFMC-28** ($E_{\text{tot}} = -9948.62 \text{ kcal/mol}$). Comparing the interaction energy (ΔE) of the Cu^{2+} and Co^{2+} (S4) ions with the framework, the results indicate that Cu^{2+} behaves strong interaction (-109.52 vs. -81.73 kcal/mol) with $\text{S}\cdots\text{O}$ chelated coordination site. This suggests that Cu^{2+} behaves strong interaction with **IFMC-28** than Co^{2+} , which is well agreement with the experimental results.

References

- 1 S. H. Mashraqui, H. Hariharasubrahmanian and S. Kumar, *Synthesis*, 1999, **12**, 2030.
- 2 S. S. Kaye, A. Dailly, O. M. Yaghi and J. R. Long, *J. Am. Chem. Soc.*, 2007, **129**, 14176.

- 3 A. R. Millward and O. M. Yaghi *J. Am. Chem. Soc.*, 2005, **127**, 17998.
- 4 G. M. Sheldrick, *SHELXL-97, Programs for X-ray Crystal Structure Refinement*; University of Göttingen: Göttingen, Germany, 1997.
- 5 (a) P. van der Sluis and A. L. Spek, *Acta Crystallogr. Sect. A*, 1990, **46**, 194; (b) A. L. Spek, *PLATON, A multipurpose crystallographic tool*, Utrecht. University, The Netherlands, 2001.
- 6 S. S. Kaye, A. Dailly, O. M. Yaghi and J. R. Long, *J. Am. Chem. Soc.*, 2007, **129**, 14176.
- 7 J. Yang, A. Grzech, F. M. Mulder and T. J. Dingemans, *Chem. Commun.*, 2011, **47**, 5244
- 8 A. D. Becke, *Phys. Rev. A*, 1988, **38**, 3098;
- 9 J. P. Perdew, *Phys. Rev. B*, 1986, **33**, 8822.
- 10 S. D. Vosko, L. Wilk and M. Nusair, *Can. J. Chem.*, 1980, **58**, 1200.
- 11 G. te Velde, F. M. Bickelhaupt, E. J. Baerends, C. Fonseca Guerra, S. J. A. van Gisbergen, J. G. Snijders and T. Ziegler, *J. Comput. Chem.*, 2001, **22**, 931.
- 12 C. Fonseca Guerra, J. G. Snijders, G. te Velde and E. J. Baerends, *Theor. Chem. Acc.*, 1998, **99**, 391.
- 13 ADF2008.01; SCM, *Theoretical Chemistry*, Vrije Universiteit: Amsterdam, The Netherlands, <http://www.scm.com>.
- 14 E. van Lenthe, E. J. Baerends and J. G. Snijders, *J. Chem. Phys.*, 1993, **99**, 4597.
- 15 E. van Lenthe, E. J. Baerends and J. G. Snijders, *J. Chem. Phys.*, 1994, **101**, 9783.
- 16 E. van Lenthe, A. E. Ehlers and E. J. Baerends, *J. Chem. Phys.*, 1999, **110**, 8943.
- 17 C. C. Pye and T. Ziegler, *Theor. Chem. Acc.*, 1999, **101**, 396.
- 18 J. L. Pascualahuir, E. Silla and I. Tunon, *J. Comput. Chem.*, 1994, **15**, 1127.
- 19 S. Z. Hu, Z. H. Zhou and K. R. Tsai, *Wuli Huaxue Xue bao*, 2003, **19**, 1073.